



## Identification of potent inhibitors of the sortilin-progranulin interaction

Shawn J. Stachel<sup>a,\*</sup>, Anthony T. Ginnetti<sup>a</sup>, Scott A. Johnson<sup>c</sup>, Paige Cramer<sup>d</sup>, Yi Wang<sup>b</sup>, Marina Bukhtiyarova<sup>b</sup>, Daniel Krosky<sup>b</sup>, Craig Stump<sup>a</sup>, Danielle M. Hurzy<sup>a</sup>, Kelly-Ann Schlegel<sup>a</sup>, Andrew J. Cooke<sup>a</sup>, Samantha Allen<sup>b</sup>, Gregory O'Donnell<sup>e</sup>, Michael Ziebell<sup>e</sup>, Gopal Parthasarathy<sup>c</sup>, Krista L. Getty<sup>e</sup>, Thu Ho<sup>e</sup>, Yangsi Ou<sup>b</sup>, Aneta Jovanovska<sup>b</sup>, Steve S. Carroll<sup>b</sup>, Mark Pausch<sup>b</sup>, Kevin Lumb<sup>e</sup>, Scott D. Mosser<sup>b</sup>, Bhavya Voleti<sup>d</sup>, Daniel J. Klein<sup>c</sup>, Stephen M. Soisson<sup>c</sup>, Celina Zerbinatti<sup>d</sup>, Paul J. Coleman<sup>a</sup>

<sup>a</sup> Department of Medicinal Chemistry, Merck & Co. Inc., PO Box 4, West Point, PA 19486, USA

<sup>b</sup> Department of Pharmacology, Merck & Co. Inc., PO Box 4, West Point, PA 19486, USA

<sup>c</sup> Department of Chemistry and Structural Chemistry, Merck & Co. Inc., PO Box 4, West Point, PA 19486, USA

<sup>d</sup> Department of Neuroscience, Merck & Co. Inc., PO Box 4, West Point, PA 19486, USA

<sup>e</sup> Screening and Protein Science, Merck & Co. Inc., PO Box 4, West Point, PA 19486, USA

### ARTICLE INFO

#### Keywords:

Sortilin  
Progranulin  
Protein-protein interaction inhibitor  
Structure activity relationship

### ABSTRACT

High-throughput screening methods have been used to identify two novel series of inhibitors that disrupt progranulin binding to sortilin. Exploration of structure-activity relationships (SAR) resulted in compounds with sufficient potency and physicochemical properties to enable co-crystallization with sortilin. These co-crystal structures supported observed SAR trends and provided guidance for additional avenues for designing compounds with additional interactions within the binding site.

Progranulin (PGRN) is a 593 amino acid secreted glycoprotein involved in development, inflammation, cell proliferation and protein homeostasis. Mutations in the granulin (*GRN*) gene, that encodes for (pro)granulin result in haploinsufficiency and reduced progranulin levels leading to the most common inherited form of frontotemporal dementia (FTD).<sup>1,2</sup> Individuals affected by this autosomal dominant trait carry loss-of-function mutations resulting in a 50% reduction in progranulin levels. In addition, *GRN*-null mutations have since been associated with other neurodegenerative phenotypes such as Huntington's, Parkinson's, and Alzheimer's Disease. Aged *GRN* knock-out (KO) mice show reduced survival, age-dependent gliosis, and increased levels of phosphorylated TDP-43 and other markers of cellular aging.<sup>3</sup> Furthermore, *GRN* KO mice display behavioral abnormalities including reduced social engagement and learning/memory deficits.<sup>4</sup> The above data suggests that reduction in progranulin levels could trigger mechanisms that are common in several neurodegenerative diseases, and that intervention which increases progranulin levels may therefore have a substantial therapeutic benefit.

Sortilin (SORT) is a type I membrane receptor, belonging to the family of vacuolar protein sorting 10 protein (VPS10P) domain receptors, that is ubiquitously expressed in both the central nervous

system and periphery.<sup>5</sup> SORT functions by shuttling proteins between the cell surface and various intracellular compartments, directing targeted proteins to distinct fates including cell surface exposure, signal transduction, regulated secretion, endocytic uptake and anterograde/retrograde sorting. PGRN binds with high affinity to SORT, resulting in its cellular uptake and eventual degradation in the lysosome.<sup>5</sup> Supportive evidence for SORT's role in controlling PGRN levels has also been demonstrated in SORT KO mice where brain and plasma PGRN levels are increased by 2.5 and 5-fold respectively.<sup>3</sup> These results indicate that inhibition of the SORT-PGRN interaction has the potential to increase PGRN levels 2.5-fold thus restoring the 50% deficit in PGRN levels observed in loss-of-function human genetic mutations causative of FTD. As such, disruption of the SORT-PGRN interaction maybe a viable therapeutic pathway for increasing progranulin levels in the CNS thereby protecting against neurodegenerative diseases including Alzheimer's Disease.

Only two small molecule protein-protein interaction inhibitors (PPIs) of the SORT-PGRN interaction have been reported in the literature to date. The Lundbeck inhibitor, AF40431 was the first such reported small molecule in the public domain, but its use as a tool molecule was limited due to low solubility and membrane permeability.<sup>7</sup>

\* Corresponding author.

E-mail address: [shawn\\_stachel@merck.com](mailto:shawn_stachel@merck.com) (S.J. Stachel).

<https://doi.org/10.1016/j.bmcl.2020.127403>

Received 1 June 2020; Received in revised form 6 July 2020; Accepted 7 July 2020

Available online 15 July 2020

0960-894X/© 2020 Elsevier Ltd. All rights reserved.

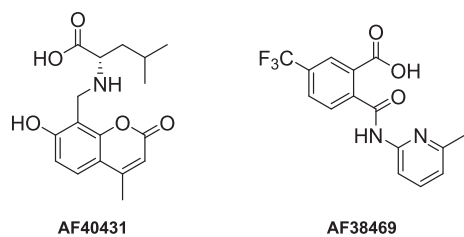


Fig. 1. Published sortilin inhibitors.

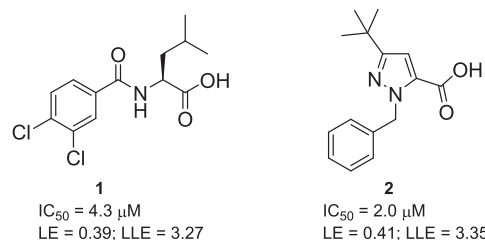


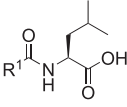
Fig. 2. HTS lead 2 and subsequent benchmark compound 1.

Lundbeck has since described AF38469 as an improved SORT-PGRN PPI with improved physicochemical properties (Fig. 1).<sup>8</sup> As part of our internal effort to identify inhibitors of the SORT-PGRN interaction, a high-throughput screen (HTS) was performed on the internal Merck compound collection using a homogeneous time-resolved fluorescence (HTRF) assay format<sup>9</sup> and subsequently confirmed as SORT binders using surface plasmon resonance (SPR). Two series, exemplified by compounds 1 and 2, emerged as promising chemotypes from a ligand binding efficiency perspective to warrant additional investigation (Fig. 2).

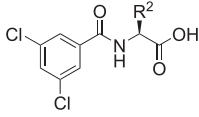
Compound 1 was identified as a singleton hit from HTS, which was notable given its relatively simple chemical structure. We began investigating the SAR by focusing on the amide as an easy handle to quickly explore this region (Table 1). Surprisingly, the amide tolerated

a widely diverse array of functionality with very little effect on activity. Variation of functional groups and positions on the aryl ring as shown in compounds 3–5 resulted in little change in potency. Likewise, extending the aryl group out by installation of a two carbon-linker as seen in compound 6 produced little effect. Introduction of charged or polar residues (compounds 7 and 8) as well as replacement of the aromatic ring with a saturated hydrocarbon (compound 9) also result in little change in activity. Most notably, even a large, saturated, polar amide such as compound 10 was within 3-fold of the simple benzamide hit 1. Given this binding data, it was the team's hypothesis that this region of the compound most likely does not interact directly with the protein, but more likely extends into solvent. As such, it was assumed that enhancement in binding affinity or potency in a ligand efficient manner would be difficult with continued exploration of this region. It was thought, however, that this region could eventually be exploited to modify the physicochemical properties of an inhibitor if additional binding potency could be realized elsewhere.

With the knowledge that we could not meaningfully increase potency through structural change in the amide region, we shifted our attention to exploration of the amino acid side chain. Keeping our most potent amide from the initial scan constant (the 3,5-dichloroamide from compound 3), we screened this region resulting in a much wider range of SAR (Table 2). Here the large cyclohexyl sidechain in 13 displayed approximately the same potency as the isopropyl sidechain, 3, whereas more subtle changes to the isopropyl group such as isopropenyl (11), cyclopropyl (12) or 1.1.1 bicyclopentane (15) lost several fold in potency. Replacement with a phenyl group (16) abrogated all activity. Interestingly, swapping from an isopropyl to a *t*-butyl group (14) resulted in an 8-fold increase in potency. Homologation to the *t*-butyl ethyl sidechain afforded an additional enhancement in potency, resulting in 17, the most potent compound in the series (IC<sub>50</sub> = 0.17 μM). However, exchanging one of the carbons for an oxygen (18) resulted in a 10-fold loss of potency and additional branching (19) led to a more dramatic loss in activity. This data led the team to the hypothesis that the amino acid sidechain is likely interacting with a more discrete pocket within the enzyme as compared with the amide region, which showed relatively flat SAR. It should be noted that activity was found to reside in the *S* enantiomer and the *R* enantiomers are inactive for all

Table 1  
Amide SAR.


Compound	R <sup>1</sup>	IC <sub>50</sub> (μM)	Compound	R <sup>1</sup>	IC <sub>50</sub> (μM)
1		4.3	7		5.3
3		2.7	8		6.3
4		4.5	9		25.3
5		6.8	10		14.4
6		6.8			

Table 2  
Amino acid SAR.


Compound	R <sup>1</sup>	IC <sub>50</sub> (μM)	Compound	R <sup>1</sup>	IC <sub>50</sub> (μM)
3		2.7	15		18
11		17.1	16		>67
12		10.7	17		0.17
13		2.3	18		1.5
14		0.35	19		>67

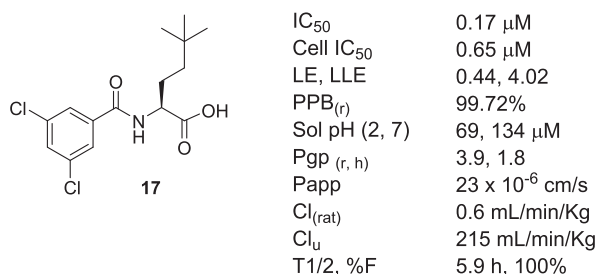


Fig. 3. Properties of Compound 17.

compounds in this series.

Because of its superior potency, we further profiled **17** to assess its utility as a potential in vivo tool molecule (Fig. 3). In addition to its activity in the biochemical assay, compound **17** also displayed sub-micromolar activity in a functional-based progranulin uptake assay<sup>9</sup> (0.65 μM). This assay measures the progranulin levels remaining in culture supernatant as measured by ELISA. Though highly protein bound in rat (99.78%), **17** displayed a good pharmacokinetic profile overall with a low unbound clearance in rat of 215 mL/min/kg,  $t_{1/2} = 5.9$  h and 100% F. Compound **17** also possessed good solubility at pH 2 and 7, good apparent permeability, was a borderline P-glycoprotein (Pgp) substrate in rat but a non-substrate against the human MDR1 cell-line, and had a clean ancillary profile with no significant responses < 10 μM in a counter-screen panel consisting of a variety of 46 enzymes and receptors.

As part of our exploratory SAR we also sought to investigate contributions of the amide and carboxylic acid to binding (Figure 4). While transformation of the acid to a primary amide or amine resulted in loss of inhibitory activity, we found that we were able to replace the carboxylic acid using tetrazole as a bioisostere (racemic compound **20**) however the modification effected a 10-fold potency loss. Additionally, we demonstrated that the carbonyl of the amide bond was not involved in a critical hydrogen bonding interaction with sortilin as replacement of the amide carbonyl with a CF<sub>3</sub> amine (**21**) resulted in only a slight loss in activity.

PGRN binds SORT in the 10-bladed β-propeller domain, resulting in cellular uptake and degradation in the lysosomes.<sup>6</sup> Neurotensin (NTS), a 13-aa neuropeptide has also been reported as a SORT ligand, binding to the same location as PGRN. The SORT-NTS complex has been determined by X-ray crystallography at 2 Å resolution.<sup>10</sup> The structure shows neurotensin binding in the 10-bladed β-propeller domain, but only the 4-C-terminal residues (10-Pro-Tyr-Ile-Leu-13) are resolved in the x-ray structure. The well-defined C-terminal region indicates its importance in SORT binding (Fig. 5).<sup>5</sup> Analysis of this structure showed a buried C-terminal salt bridge interaction with Arg292 with additional bifurcating hydrogen-bond interactions with Tyr318 and Ser283, the hallmark salt bridge. In addition to the salt bridge interaction, the leucine sidechain can be seen nestled into a small hydrophobic pocket. Hydrogen bond interactions are also present between the pocket and the terminal amide of NTS, as well as hydrogen bonding interactions between the hydroxyl group of Tyr318 and Lys227 of SORT. The

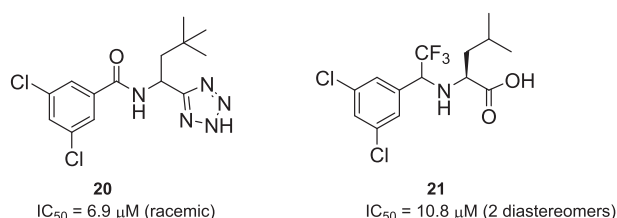
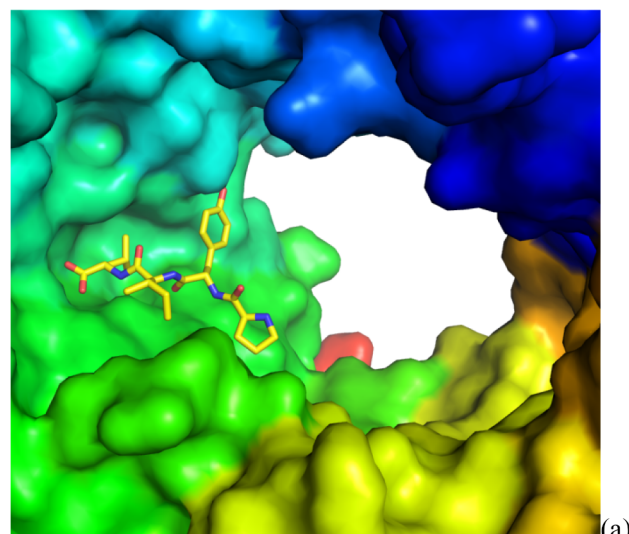
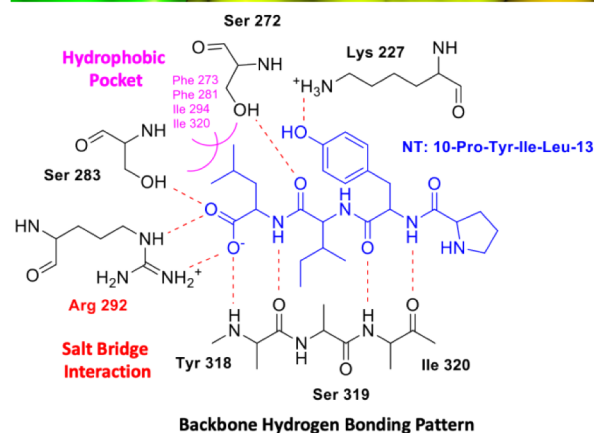


Fig. 4. Compound 17 bioisostere replacements.



(a)



(b)

Fig. 5. NTS binding interactions with SORT receptor.

importance of these terminal amino acids for binding has also been demonstrated experimentally where truncation of the five c-terminal (Leu-Arg-Glu-Leu-Leu) residues from full-length progranulin peptide completely eliminated its ability to be endocytosed by SORT.<sup>11</sup>

We co-crystallized compound **17** with SORT and showed that it also binds to the NTS/PGRN binding site (Fig. 6). As seen in the co-crystal with neurotensin, compound **17** is also anchored through a salt bridge with Arg292 and additional interaction with Ser283 and Tyr318. In addition, the *t*-butylethyl sidechain occupies the same hydrophobic

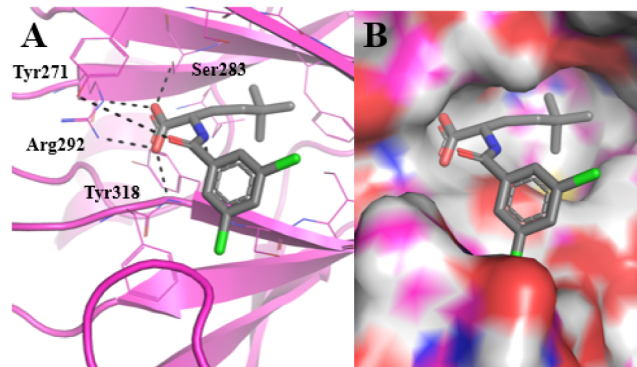


Fig. 6. Co-crystals structure of compound **17** in the SORT binding pocket. (A) indicates key hydrogen bonding interactions (black dashes) between compound **17** (grey) and the protein (pink). (B) Protein molecular surface representation. PDB ID: 6X48.

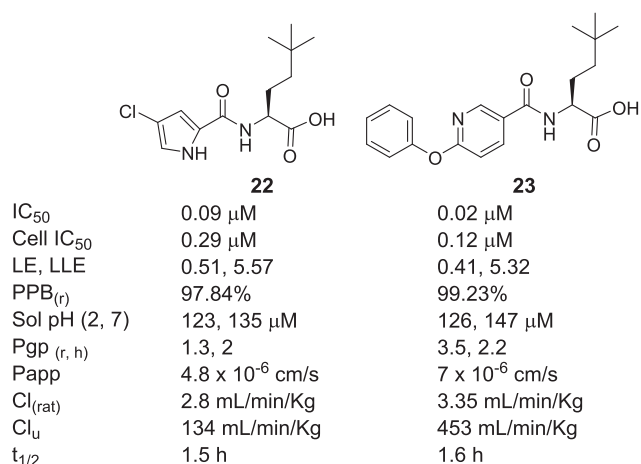


Fig. 7. Optimized compounds in amide series.

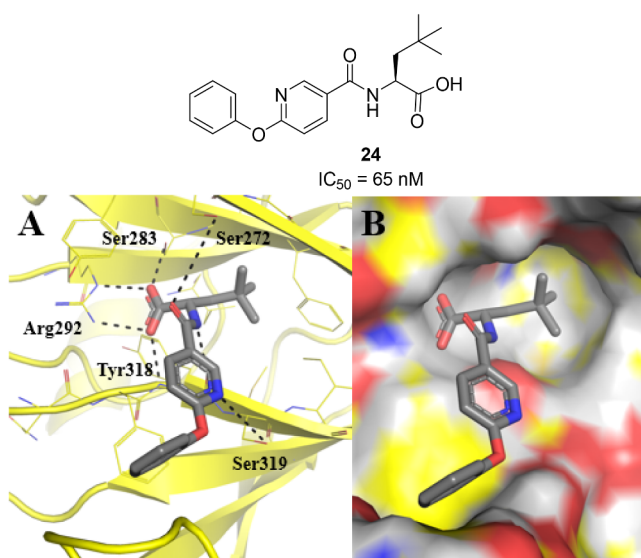


Fig. 8. Co-crystals structure of compound 24 in the SORT binding pocket. (A) indicates key hydrogen bonding interactions (black dashes) between compound 24 (grey) and the protein (yellow). (B) Protein molecular surface representation. PDB ID: 6X4H.

pocket as the leucine sidechain in neurotensin. The aryl ring, however, is orientated into the central solvent exposed cavity of the sortilin channel. The lack of hydrophobic interactions with the protein here potentially explain the promiscuity observed in the flat SAR for this region.

The crystallographic data also supported the result obtained with compound 21, where the amide was replaced with  $\alpha$ -CF<sub>3</sub> amine, confirming that the carbonyl oxygen was not involved a direct hydrogen-bonding interaction with the protein. This is in contrast to the amide carbonyl of NTS, which is observed to hydrogen bond to Ser272 in the SORT-NTS x-ray structure. These structural results spurred a re-investigation of the amide with the hypothesis that binding might be enhanced through more distal interaction with the progranulin binding site as observed with neurotensin. As such, we re-explored the amide region again, this time using the optimized *t*-butylethyl amino acid side chain.

Upon a second iteration of amide screening, we were able to affect additional improvements in activity whilst retaining the favorable physicochemical properties present in compound 17 as shown with compounds 22 and 23 (Fig. 7). These improvements in potency are also commensurate with increases in lipophilic ligand efficiency (LLE), 5.57

Table 3  
SAR for pyrazole benzyl region.

Compound	R <sup>1</sup>	IC <sub>50</sub> (μM)	Compound	R <sup>1</sup>	IC <sub>50</sub> (μM)
2		2.0	28	Me	8.3
25		2.1	29		7.6
26		3.0	30		5.3
27		2.1	31		0.49

and 5.32 for compounds 22 and 23 respectively vs. 4.02 for compound 17. These findings are particularly noteworthy given that the increased potency is comparable with the intrinsic activity of the 18-mer PGRN peptide, IC<sub>50</sub> = 0.014 μM, which issued as the positive control in the assay. In addition to the improvements in activity, compounds 22 and 23 also possessed favorable pharmacokinetic profiles with low unbound clearance in rat, good solubility at pH 2 and 7, and Pgp efflux ratio suitable for CNS penetration although the apparent permeability for these analogs was somewhat reduced compared to 17.

The improvement in potency observed in compound 23 can be rationalized by analyzing the co-crystal of a similar compound 24, in the SORT binding site where the homo *t*-butyl group is replaced by a *t*-butyl leucine. Fig. 8 shows that additional hydrophobic interactions are present in an edge-to-face  $\pi$ -interaction of the terminal aryl ring with Tyr362, as well as a face-to-face  $\pi$ -interaction between the pyridyl ring and Phe317. Two additional interactions are also observed: a direct hydrogen-bonding interaction between the aryl ether oxygen and the Tyr362 phenol as well as a bidentate water-mediated hydrogen-

Table 4  
SAR in 3-position of pyrazole series.

Compound	R <sup>1</sup>	R <sup>2</sup>	IC <sub>50</sub> (μM)
2		Phenethyl	2.0
32		benzyl	6.6
33		Phenethyl	>67
34		benzyl	>67

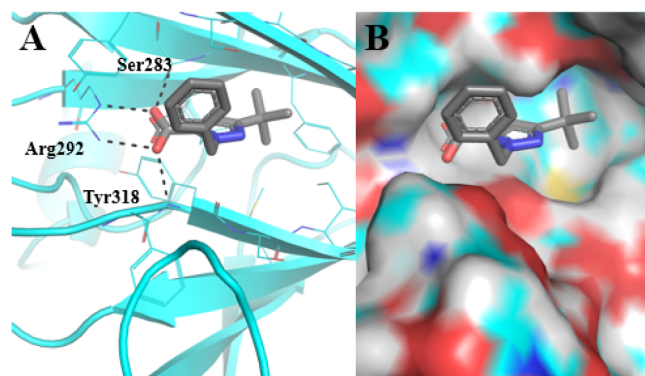


**Fig. 9.** Co-crystals structure of compound **2** in the SORT binding pocket. (A) indicates key hydrogen bonding interactions (black dashes) between compound **2** (grey) and the protein (cyan). (B) Protein molecular surface representation. PDB ID: 6X3L.

bonding interaction between the aryl ether and the Tyr362 carbonyl and phenol.

Compound **2** represents a second series that was identified in our HTS campaign. We began our investigation of this second series by focusing on the benzyl portion of the molecule. As was observed in the amide portion of the first series, the SAR was very flat with a wide diversity of size and polarity resulting in little effect on potency as shown in Table 3. By contrast the *t*-butyl group showed much less tolerability for modification (Table 4) as compared to the previous amide series. In light of the structural similarities between the two series (*t*-butyl, carboxylic acid moieties) we sought to determine if homologation of the *t*-butyl group would prove beneficial as it had previously. Unfortunately, these modifications resulted in reduced potency.

Again, co-crystallographic analysis of the inhibitor-SORT complex with 2.7 Å resolution provided additional insight. The crystal structure showed, unsurprisingly, that this series indeed binds in the same site on SORT as the previous series with similar interactions (Fig. 9). The carboxylic acid was involved in a hydrogen bonding network with Arg292, Ser283, and Tyr318, and the *t*-butyl group occupied the hydrophobic binding pocket occupied by the leucine in NTS and compound **17**. Again, the benzyl group was oriented into the solvent exposed central cavity of the SORT channel thereby explaining the flat SAR, as was observed in the amide series. However, in this instance, the benzyl substituent was orientated upwards, thereby limiting access to potentially engaging additional binding interactions as realized in compound **23** as compared to **27**. The most active analog obtained in this series was compound **31** with and  $IC_{50} = 0.49 \mu\text{M}$ . While it was

initially hypothesized that these structurally distinct HTS hits that appeared to share common functional groups might bind in similar locations, it is reassuring nonetheless that the convergent SAR and binding validation by co-crystallization confirmed these assumptions.

In summary, we have identified two novel inhibitor series of the SORT-PGRN interaction via high-throughput screening. Initial SAR resulted in compounds with improved potency and physicochemical properties enabling co-crystallization with SORT. These co-crystal structures supported the SAR and provided guidance for additional avenues for increased interactions within the binding site. These two series were found to share a common binding motif anchored by a carboxylate-arginine salt bridge that is also critical in PGRN binding to the SORT receptor. Further optimization of these series and in vivo pharmacodynamic studies will be the subject of a future publication.

**Supporting Information:** Experimental procedures and compound characterization data for lead compounds. The Supporting Information is available free of charge on the ACS Publications website. Structure coordinates have been deposited in the Protein Data Bank (PDB): codes 6X48, 6X4H, 6X3L.

### Declaration of Competing Interest

The authors declare that they have no known competing financial interests or personal relationships that could have appeared to influence the work reported in this paper.

### Appendix A. Supplementary data

Supplementary data to this article can be found online at <https://doi.org/10.1016/j.bmcl.2020.127403>.

### References

- Eriksen JL, Mackenzie RA. *J. Neurochem.* 2008;104:287–297.
- Riedl L, Mackenzie IR, Forstl H, Kurz A, Diehl-Schmid J. *Neuropsychiatr Dis Treat.* 2014;10:297–310.
- Kumar-Singh S. *J. Mol. Neurosci.* 2011;45:561–573.
- Arrant AE, Filiano AJ, Warmus BA, Hall AM, Roberson ED. *Genes Brain Behavior.* 2016;15:588–603.
- Petersen CM, Nielsen MS, Nykjaer A, et al. *J. Biol. Chem.* 1997;272:3599–3605.
- Hu F, Padukkavidana T, Vægter CB, et al. *Neuron.* 2010;68:654–657.
- Andersen JL, Schröder TJ, Christensen S, et al. *Acta Cryst.* 2014;D70:451–460.
- Schröder TJ, Christensen S, Lindeberg S, et al. *Bioorg. Med. Chem. Lett.* 2014;24:177–180.
- Experimental conditions and procedures for the HTRF and functional-based progranulin uptake assays are described in the Supporting Information section.
- Quistgaard, E. M.; Madsen, P.; Grøftehauge, M. K.; Nissen, P.; Claus M Petersen, C. M.; Søren S Thirup, S. S. *Nat. Struct. Mol. Biol.* 2009, 16, 96–98.
- Lee WC, Almeida S, Prudencio M, et al. *Hum Mol Genet.* 2014;23:1467–1478.